Special Feature: GaN for Opto- and Power-electronic Applications (1)

General features of GaN-related materials

Katsuhiko Inaba*

1. Introduction

In modern society where our daily environment is supported by various electronic devices, it is critical to pursue opto-electronic or power-electronic devices with less environment impact and with higher efficiency of energy conversion to ensure a sustainable society. GaN (gallium nitride) and related materials have been a focus of attention for the issue of sustainability.

Rigaku has been receiving a large number of questions concerning characterization techniques of GaN and related materials. Rigaku's investigation led to the conclusion that there exist specific difficulties inherent in the characterization of GaN related materials. Some of them originate from the uniqueness of the crystallographic features of GaN, and some of them are inherent to the heteroepitaxial growth of GaN films with huge lattice mismatches.

These findings were a motivation to produce a special article for the Rigaku Journal to review and highlight the topics in the characterization techniques of GaN-related materials, that show promise for optoelectronic and power electronic applications. In this article, general features of the crystallographic nature of GaN-based materials are discussed. Recent topics concerning XRD characterization techniques are the subject of the next article.

2. What is "GaN" ?

It is interesting to start with a historical perspective. At a scientific meeting in mid-1990s, the main topics of discussion were related to blue light emitting devices in the future. Four kinds of promising materials or techniques were talked about at that meeting.

1. GaN-based III–V nitride compound semiconductors
2. ZnSe-based II–VI compound semiconductors
3. Wavelength conversion by higher order harmonic generation using non-linear optical crystals
4. Up-conversion emission of shorter wavelength light pumped by longer wavelength light

Epitaxial growth of GaN films on sapphire substrates has progressed dramatically since the mid-1990's. The lack of native GaN substrates was reported as one of the original difficulties of GaN growth with high crystalline quality. A GaN bulk single crystal can be obtained only under extreme high pressure conditions of several tens of kilo bars(1),(2). Therefore, GaN epitaxial films were grown on sapphire substrates in spite of the large lattice mismatches between them. In this respect, ZnSe (zinc selenide) has an advantage over GaN, since bulk single crystals of ZnSe were obtained using the Bridgman technique, which had been applied to manufacturing large-sized bulk GaAs (gallium arsenide) single crystals.

Dramatic improvements in crystalline quality of GaN epitaxial films on foreign substrates with large lattice mismatches have been brought about by the introduction of low temperature buffer layers(3) or other techniques.

It is interesting to make a comparison of GaN-based blue light emitting materials with the market-leading GaAs-based red light emitting materials.

2.1. GaN epitaxial growth on foreign substrates

For Gaas-based materials to be used in red light emitting laser applications, solid solutions (also called "the mixed crystals") of compound semiconductor materials with different compositions, such as (Al, Ga)As, are grown epitaxially on GaAs single crystal substrates. Due to the difference of their compositions, their lattice constants differ according to their compositions, but the differences are generally less than 1%. Moreover, though the growth of these compounds is classified as heteroepitaxial growth, the crystal structure of all these compounds is a zincblende-type crystal structure with cubic symmetry.

GaN growth on Sap or on Si is also classified as one of heteroepitaxial growth. There exists a big mismatch between GaN-based materials and sapphire or Si. So-called mismatches are approximately 16% for GaN on sapphire, and approximately 17% for GaN on Si substrate. Both the sapphire substrate crystal (corundum-type structure, rhombohedral symmetry) and the Si substrate crystal (diamond-type structure, cubic symmetry) are crystal structures totally different from GaN (wurtzite-type structure, hexagonal symmetry). Therefore, lattice matching cannot be simply discussed with the difference of lattice constants, but should be discussed with respect to the differences of lattice spacing within the planes of interfaces, where the matching of atomic arrangements should be taken into consideration. A typical crystallographic orientation relationship in the case of *c*-axis growth GaN epitaxial film on the sapphire (0001) substrate is shown in Fig. 1. The atomic arrangements of the *c*-plane of sapphire and the *c*-plane of GaN are shown in Fig. 2. Atomic arrangements to be matched are showed by

---

* X-ray Research Laboratory, Rigaku Corporation.

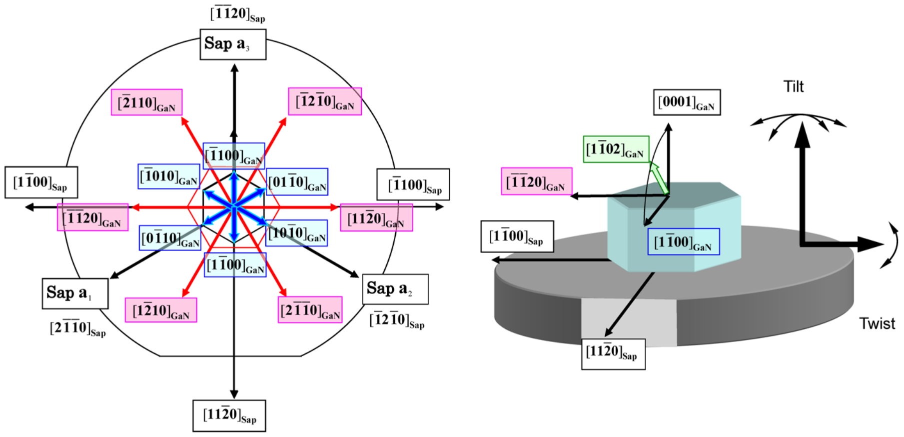

Fig. 1. Orientational relationship of GaN epitaxial films on sapphire (0001) substrate.

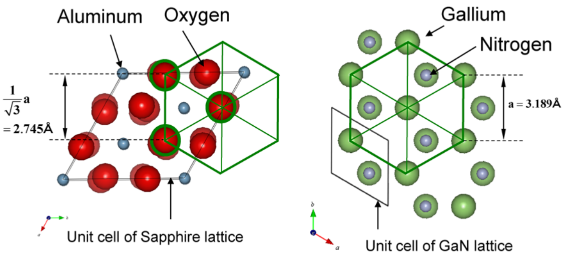

Fig. 2. Atomic arrangements of **c**-plane of sapphire and GaN.

green hexagons. Oxygen atoms with different fractional coordinates are included in the figure of *c*-plane sapphire (the left figure of Fig. 2.) However, oxygen atoms lying on the interfacial planes are marked with green circles. In addition, a typical crystallographic orientation relationship for the *c*-axis growth GaN epitaxial film on the Si(111) substrate is shown in Fig. 3. The epitaxial orientation relationships are expressed as follows.

$[11\bar{2}0](0001)\mathrm{GaN}//[1\bar{1}00](0001)\mathrm{Sap}$
(or, $[1\bar{1}00](0001)\mathrm{GaN}//[11\bar{2}0](0001)\mathrm{Sap}$)
$[11\bar{2}0](0001)\mathrm{GaN}//[1\bar{1}0](111)\mathrm{Si}$
(or, $[1\bar{1}00](0001)\mathrm{GaN}//[11\bar{2}](111)\mathrm{Si}$)

One parameter that came to be a focus of attention with respect to crystalline quality of the GaN epitaxial film was the twisting of the mosaic spread(4)–(8).

The crystalline quality of (Al,Ga)As epitaxial films on GaAs substrates was generally evaluated only with the tilting of mosaic spread, which was defined as the degree of the orientation variation (the orientation disorder along the growth direction) along the growth axis of epitaxial films. However, in the case of GaN epitaxial films where large mismatches exist between films and substrates, their crystalline quality cannot be sufficiently evaluated only from the tilting of the mosaic spread. In addition to the tilting of mosaic spread, the twisting of mosaic spread (the orientation disorder within the interfacial planes) is also an important parameter to characterize the crystalline quality of GaN epitaxial films (see Fig. 1).

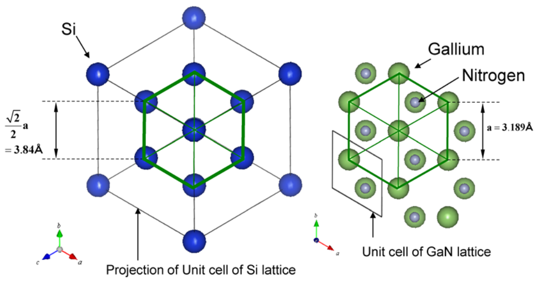

Fig. 3. Atomic arrangements of (111) Si and **c**-plane of GaN.

Furthermore, due to the nature of epitaxial growth on the different kinds of substrate, the following issues need to be discussed also.

2.1.1. Misorientations

A slight misorientation between the lattices of epitaxial films and those of substrates along the growth direction is often reported for the epitaxial growth of GaN-based materials. In recent years, the misorientation within interfacial planes (mis-alignment of lattices between films and substrates within the interfacial planes) came to be recognized as an important parameter for the evaluation of required crystalline quality(4),(9)–(11).

Great efforts have been made to overcome these great mismatches between films and substrates. As a consequence, the introduction of miscut substrates has been tried(12), where their surface planes were intentionally inclined during the slicing process of the substrate boules. A careful characterization of misorientations in these systems is necessary.

2.1.2. Elastic lattice distortion

Epitaxial growth films are constrained to substrates, and thus, are often accompanied by elastic lattice distortion depending on mismatch. There exists a practical need to evaluate the composition (atomic ratio) of epitaxial films by X-ray diffraction techniques. From X-ray diffraction, the composition of materials can be estimated from a planar spacing of lattices. But the variation of lattice spacing is impacted by lattice distortion. The reciprocal space map (RSM) measurement is often used for the purpose of evaluating the degree of the lattice distortion(6),(13)–(15). From the RSM measurements, the information of the position of the diffraction signal (reflection) can be evaluated, and then the contribution of variation of lattice constants and the degree of lattice distortion can be analyzed independently. The separation of these contributions can be done only after the degree of lattice misorientation is clearly identified (see former paragraph).

2.1.3. Mismatch in thermal expansion

There is a difference in the thermal expansivity between a substrate and the epitaxial film because the crystal structures are different. This is important because there is a large change in temperature during the cooling process to room temperature from the growth condition (generally around 1,000°C). Therefore, epitaxial films suffer with another "lattice distortion" caused by thermal stress caused by the mismatch of thermal expansion coefficients. The curvature of these materials is also reported as one of the crucial obstacles for device fabrication. Physical parameters, such as lattice constants, thermal expansion coefficients, elastic stiffness coefficients for GaN-related materials (GaN, AlN, InN, Sap, Si, ZnO) reported in various articles are summarized in Tables 1 to 3.

The value of the linear thermal expansion coefficient of the *a*-axis of GaN is between the one of sapphire and Si. After growth at high temperature, a *c*-axis grown GaN film on a *c*-plane Sap will suffer from the compressive stress within an interface plane. This is because the thermal contraction along the *a*-axis (within the interface plane) of the sapphire is bigger than that of GaN. On the contrary, tensile stress will act on a GaN film grown on Si (111), because of the smaller thermal contraction of the Si substrate within the interfacial plane due to the thermal expansion of GaN being bigger than that of Si.

The curvature is also reported in samples where thick buffer layers are introduced. This curvature is convex in the case of GaN epitaxial films grown on sapphire substrates, and is concave in the case of GaN epitaxial films grown on Si substrates. The difference of signs of curvature is reasonably explained from the difference of thermal expansions between GaN films and substrates(16). The curvature of samples is sometimes evaluated by the laser interferrometry as the morphology of surface. But it is better and more precise to evaluate the degree of curvature directly from the curvature of lattices of substrates using XRD.

2.2. Complexity originating from the nature of crystal structures

The crystal structure of GaN is known to be a wurtzite-type structure, the same as ZnO. This crystal structure type belongs to a system with hexagonal symmetry, where principle axes of a_1-axis and a_2-axis intersect with each other at 120 degrees, whereas the intersecting angle with *c*-axis and a_1-axis or a_2-axis is rectangular. Therefore, symmetry around the *c*-axis of GaN as a growth direction shows six-fold symmetry. The notations of the crystallographic axes or lattice planes are very complex if compared to the notations for cubic systems (see Figs. 1–3).

Table 1. Lattice constants for GaN-related materials.

	a (Å)	*c* (Å)	*u*-parameter	Remarks	Ref
GaN	3.1896	5.1855	—	free-standing GaN by LEO	25
	3.189	5.185	—		26
	3.18926	5.18523	—	HVPE bulk GaN	27
	3.190	5.189	0.377	single crystal XRD	28
AlN	3.112	4.982	—		26
	3.110	4.980	0.3821	single crystal XRD	28
InN	3.545	5.703	—		26
	3.537	5.703	—		29
	3.540	5.706	0.380		30
Si	5.43102			powder XRD	31
	5.43159			powder XRD	32
Sap	4.75916	12.99212		powder XRD	33
	4.7617	12.9990		single crystal XRD	34
ZnO	3.2496	5.2042	0.3819		35
	3.2501	5.2071	0.3817		36

"*u*-parameter" denotes fractional coordinates for anions in the *c*-axis direction in the unit cell of wurtzite structure.

Table 2. Thermal expansion coefficients for GaN-related materials.

	α_a	α_c	Remarks	Ref
GaN	3.43×10^{-6}	3.34×10^{-6}	powder	37
	3.1×10^{-6}	2.8×10^{-6}	single crystal	38
	3.8×10^{-6}	2.0×10^{-6}	epitaxial thinfilm sample	38
	5.59×10^{-6}	3.17×10^{-6}	epitaxial thinfilm sample	39
AlN	4.35×10^{-6}	3.48×10^{-6}	powder	37
	2.8×10^{-6}	2.7×10^{-6}	single crystal, data taken from the figure	40
InN	4×10^{-6}	3×10^{-6}		41
	3.6×10^{-6}	2.6×10^{-6}	nanocrystalline powder	42
	3.83×10^{-6}	2.75×10^{-6}	theoretical calculation	29
Si	2.618×10^{-6}			43
Sap	6.06×10^{-6}	6.19×10^{-6}	single crystal	34
	5.46×10^{-6}	5.69×10^{-6}	powder	33
	4.3×10^{-6}	3.9×10^{-6}		38
ZnO	6.11×10^{-6}	3.59×10^{-6}		44
	4.31×10^{-6}	2.49×10^{-6}	powder	37

(at room temperature)

Table 3. Values of elastic stiffness coefficients for GaN-related materials.

	C_{11}	C_{12}	C_{13}	C_{14}	C_{33}	C_{44}	Remarks	Ref
GaN	296	130	158		267	24	polycrystalline sample, temperature dependency	41, 45
	367	135	103		405	95	theoretical calculation	46
	373	141	80.4		387	93.6	free-standing GaN by LEO, Brillouin spectroscopy	25
	370	145	106		398	105	GaN on Sap, SAW measurement	47
	377	160	114		209	81.4	free-standing GaN by HVPE, resonant ultrasonic spectroscopy	48
	390	145	106		398	105	needle-like single crystal, Brillouin spectroscopy	49
	359.4	129.2	92		389.9	98.0	single crystal, resonant-ultrasound spectroscopy	50
AlN	396	137	108		373	116	theoretical calculation	46
	411	149	99		389	125	single crystal, data taken from the figure	51
	410	140	100		390	120	AlN on Sap, SAW measurement	47
InN	190	104	121		182	10		41
	223	115	92		224	48	theoretical calculation	46
Si	167.4	65.23				79.57		52
	165.64	63.94				79.51		53
Sap	497	163	116	22	501	147	polycrystalline sample	54
	497.5	162.7	115.5	22.5	503.3	147.4	single crystal	55
	497.1	164.7	129.5	18.6	492.5	154.2	LDA calculation	56
ZnO	209.7	121.1	105.1		210.9	42.5	single crystal, ultrasonic	57
	190	110	90		196	39	single crystal, polarized Brillouin scattering	58
	157	89	83		208	38	thinfilm, acoustic investigation	59

(in GPa units)

However, the symmetry around the *c*-axis of sapphire or [111] axis of Si shows a three-fold symmetry, in which an equivalent direction appears every 120 degrees around the corresponding axis. (note: the crystal lattice of Sap is normally shown with the hexagonal lattice because of the convenience of expression. But, it should be noted that its lattice has rhombohedral symmetry.) The understanding of this difference of symmetry between GaN-based films and substrates will be helpful in case of measuring RSMs of asymmetric lattice planes.

A wurtzite-type structure does not have an inversion center of symmetry (this is called "noncentrosymmetric"). This feature implies that a GaN single crystal has "crystallographic polarity", and thus, exhibits piezoelectric and pyroelectric effects. Since this polarity is designated along its *c*-axis direction, some of its physical properties will be different whether the crystal is directed to the +*c* direction or to the −*c* direction. In the case of GaN, the +*c* direction or the –*c* direction is also expressed as the Ga -polar direction or N (nitrogen) -polar direction, respectively. The influences of polar axes are canceled out within lattice planes parallel to these polar axes (for example, *a*-planes; $\{11\bar{2}0\}$, or *m*-planes; $\{1\bar{1}00\}$), these lattice planes are called non-polar planes. The lattice planes intersecting polar axes with an oblique angle other than 90 degrees, where the influences of polar direction are partially compensated, are called semi-polar lattice planes. It may be worth mentioning that the zincblende-type crystal structure is also a noncentrosymmetric structure. Based on the difference of crystallographic polarity, {111} lattice planes of zincblende-type structures, for example GaAs, are identified as (111)A or (111)B because the polar axis is <111>. The intrinsic electric field is influenced with spontaneous and piezoelectric polarization. Therefore, the performance of opto-electronic or power-electronic devices based on GaN-based materials should be crucially correlated with device designs to stack the GaN-related films via their polarity direction.

Not only the bulk material, but also the surface atoms are greatly governed by the crystallographic polarity. So, the growth rate or the rate of impurity accumulation into the lattice has a high correlation with the polarity of the growth direction of films.

In order to suppress or minimize the influence of the spontaneous and piezoelectric polarization within multilayered structures of GaN-based materials, the fabrication of layer structures along the non- or semi-polar directions has been closely studied in recent years.

Heat dissipation from the device structure is one of the problems that need to be solved. Therefore the analysis with high-temperature XRD might be an informative method for examining the degradation of the layer structures of the true device. The gas desorption analysis may work well for characterization of the volatile constituents or the residues of the supplied source materials in the growth by HVPE or MOCVD techniques, or of the desorption from the surface electrodes.

3. Hot Topics

As mentioned in the previous section, GaN-based multi quantum well (MQW) layer structures grown along the polar *c*-axis suffer greatly with spontaneous or piezoelectric polarization leading to a drop of internal quantum efficiency of light emission, or fatally leading to the degradation of layer structures. One of the approaches to solve these problems is the growth of GaN in the non- or semi-polar direction. The growth of non- or semi-polar GaN are successful using ZnO substrates, *r*-plane sapphire substrates, Si(113) substrate, *m*-plane SiC substrates, *a*-plane of γ-LiAlO$_2$ substrates, etc.

The determination of the crystallographic polar direction has been done by characterization techniques such as etching or the electron beam diffraction. It should be noted that the determination of the crystallographic polar direction is also possible by the X-ray diffractometry(17). Explanations of this characterization technique will be done in the next article.

Large demand for native GaN substrates drives the progress of GaN single crystal growth in size and quality(18), as the thick film growth by the HVPE method(19),(20) or the large-sized bulk growth by the ammonothermal method(1),(21), or the bulk crystal growth at low temperature using the flux growth method(22)–(24). In growing bulk single crystals, a flux (Na or Li) and a mineralizer are used for the promotion of crystal growth. In the case of high-speed thick film growth by the HVPE method, there remains a feasibility of absorption of carrier gas elements to the crystal body. Elemental analyses such as total-reflection X-ray fluorescence (TXRF) analysis, secondary-ion mass spectroscopy (SIMS), and glow discharge emission spectrometry will work well to analyze the impurity elements left in the crystal body, or to trace the possibility of elemental interdiffusion across the MQW structures or the interfacial reaction between the electrodes and MQWs.

4. Summary

General crystallographic features in GaN-related materials were briefly discussed based on the two characteristics of GaN-related materials; “GaN epitaxial growth on foreign substrates” and “complexity originating from the nature of the crystal structure”. A clear understanding of these issues are indispensable for the characterization of GaN-based epitaxial films to be used in optoelectronic and power electronic applications.

In the next article, a characterization technique using high-resolution (HR) XRD will be focused. The HR-XRD technique became popular in the course of being employed as a characterization technique for GaAs-based epitaxial films. But it should be kept in mind the significant difference in the crystallographic properties between GaN-based materials and GaAS-based materials. The intention of this article was to act as preparation to start the discussion of HR-XRD characterization of GaN epitaxial films by briefly reviewing their features specific to GaN-based materials. It is hoped that these articles will assist our reader’s research activity.

Finally, it is hoped that the technical issues shown in the present article can be analogously applied to the characterization of new functional materials in the future.

References

(1) T. Fukuda and D. Ehrentraut: *Jour. Cryst. Growth*, **305** (2007), 304–310.

(2) J. Karpinski, J. Jun and S. Porowski: *Jour. Cryst. Growth*, **66** (1984), 1–10.

(3) H. Amano, N. Sawaki, I. Akasaki and Y. Toyoda: *Appl. Phys. Lett.*, **48** (1986), 353–355.

(4) S. Kobayashi: *Rigaku Journal* (*English version*), **26** (2010), No. 1, 3–11.

(5) M. E. Vickers, M. J. Kappers, R. Datta, C. McAleese, T. M. Smeeton, F. D. G. Rayment and C. J. Humphrey: *J. Phys. D: Appl. Phys.* **38** (2005), A99–A104.

(6) O. Ambacher: *J. Phys. D: Appl. Phys.*, **31** (1998), 2653–2710.

(7) Y. J. Sun, O. Brandt, T. Y. Liu, A. Trampert and K. H. Ploog, J. Bläsing and A. Krost: *Appl. Phys. Lett.*, **81** (2002), 4928–4930.

(8) Y. Zoo, N. D. Theodore and T. L. Alford: *Jour. Appl. Phys.*, **102** (2007), 083545-1–083545-6.

(9) S. Keller, N. A. Fichtenbaum, F. Wu, D. Brown, A. Rosales, S. P. DenBaars, J. S. Speck and U. K. Mishra: *Jour. Appl. Phys.*, **102** (2007), 083546-1–083546-7.

(10) H. K. Chauveau, P. De Mierry, H. Cabane and D. Gindhart: *Jour. Appl. Phys.*, **104** (2008), 113516-1–113516-7.

(11) Y. Zhang, C. McAleese, H. Xiu, C. J. Humphreys, R. R. Lieten, B. Degroote and G. Borghs: *Appl. Phys. Lett.*, **91** (2007), 092125-1–092125-2.

(12) T. Yuasa, Y. Ueta, Y. Tsuda, A. Ogawa, M. M. Taneya and K. Takano: *Jpn. Jour. Appl. Phys.*, **38** (1999), L703–L705.

(13) S. Pereira, M. R. Correia, E. Pereira, K. P. O’Donnell, E. Alves, A. D. Sequeira, N. Franco, I. M. Watson and C. J. Deatcher: *Appl. Phys. Lett.*, **80** (2002), 3913–3915.

(14) F. Oehler, M. E. Vickers, M. J. Kappers and R. A. Oliver: *Jour. Appl. Phys.*, **114** (2013), 053520-1–053520-11.

(15) T. Konya: *Rigaku Journal* (*English version*), **25** (2009), No. 2, 1–8.

(16) T. Paskova, L. Becker, T. Böttcher, D. Hommel, P. P. Paskov and B. Monemar: *Jour. Appl. Phys.*, **102** (2007), 123507-1–13507-4.

(17) K. Inaba and H. Amano: *Phys. Stat. Sol. -B*, **44** (2007), 1775–1779.

(18) H. Amano: *Jpn. Jour. Appl. Phys.*, **52** (2013), 050001-1–050001-10.

(19) K. Fujito, K. Kiyomi, T. Mochizuki, H. Oota, H. Namita, S. Nagao and I. Fujimura: *Phys. Stat. Sol. -A*, **205** (2008), 1056–1059.

(20) Y. Kagamitani, D. Ehrentraut, A. Yoshikawa, N. Hoshino, T. Fukuda, S. Kawabata and K. Inaba: *Jpn. Jour. Appl. Phys.*, **45** (2006), 4018–4020.

(21) R. Kucharski, M. Zając, R. Doradziński, M. Rudziński, R. Kudrawiec and R. Dwiliński: *Semicond. Sci. Technol.*, **27** (2012), 024007.

(22) M. Imanishi, K. Murakami, H. Imabayashi, H. Takazawa, Y. Todoroki, D. Matsuo, M. Maruyama, M. Imade, M. Yoshimura

and Y. Mori: *Phys. Stat. Sol. -C*, **10** (2013), 400–404.

(23) X. L. Chen: *Sci. Tech. Adv. Mater.*, **6** (2005), 766–771.

(24) M. Aoki, H. Yamane, M. Shimada, S. Sarayama and F. J. DiSalvo: *Jour. Cryst. Growth*, **242** (2002), 70–76.

(25) T. Deguchi, D. Ichiryu, K. Toshikawa, K. Sekiguchi, T. Sota, R. Matsuo, T. Azuhata, M. Yamaguchi, T. Yagi, S. Chichibu and S. Nakamura: *Jour. Appl. Phys.*, **86** (1999), 1860–1866.

(26) I. Vurgaftman and J. R. Meyer: *Jour. Appl. Phys.*, **94** (2003), 3675–3696.

(27) V. Darakcieva, B. Monemar and A. Usui: *Appl. Phys. Lett.*, **91** (2007), 031911-1–031911-3.

(28) H. Schulz and K. H. Thiemann: *Solid State Commun.*, **23** (1977), 815–819.

(29) K. Wang and R. R. Reeber: *Appl. Phys. Lett.*, **79** (2001), 1602–1604.

(30) P. Rinke, M. Winkelnkemper, A. Qteish, D. Bimberg, J. Neugebauer and M. Scheffler: *Phys. Rev. -B*, **77** (2008), 075202-1–075202-15.

(31) The NIST Reference on Constants, Units and Uncertainty (*http://physics.nist.gov/cuu/index.html*).

(32) D. R. Black, D. Windover, A. Henins, D. Gil, J. Filliben and J. P. Cline: *Powder Diffraction*, **5** (2010), 187–190.

(33) T. Mitsunaga, M. Saigo and G. Fujinawa: *Powder Diffraction*, **17** (2002), 173–177.

(34) S. Kondo, K. Tateishi and N. Ishizawa: *Jpn. Jour. Appl. Phys.*, **47** (2008), 616–619.

(35) H. Karzel, W. Potzel, M. Köfferlein, W. Schiessl, M. Steiner, U. Hiller, G. M. Kalvius, D. W. Mitchell, T. P. Das, P. Blaha, K. Schwarzand and M. P. Pasternak: *Phys. Rev. -B*: **53** (1996), 11425–11438.

(36) E. Kisi and M. M. Elcombe: *Acta Cryst. -C*, **45** (1989), 1867–1870.

(37) H. Iwanaga, A. Kunishige and S. Takeuchi: *Jour. Mater. Sci.*, **35** (2000), 2451–2454.

(38) M. Leszczynski, T. Suski, H. Teisseyre, P. Perlin, I. Grzegory, J. Jun, S. Porowski and T. D. Moustakas: *Jour. Appl. Phys.*, **76** (1994), 4909–4911.

(39) H. P. Maruska and J. J. Tietjen: *Appl. Phys. Lett.*, **15** (1969), 327–329.

(40) H. Kröncke, S. Figge, B. M. Epelbaum and D. Hommel: *Acta Physica Polonica -A*, **114** (2008), 1193–1200.

(41) A. U. Sheleg and V. A. Savastenko: *Vesti Akad. Nauk BSSR, Ser. Fiz. Mater. Nauk* **3** (1976), 126.

(42) W. Paszkowicz, J. Adamczyk, S. Krukowski, M. Leszczyński, S. Porowski, J. A. Sokolowski, M. Michalec and W. Łasocha: *Phil. Mag.*, **79** (1999), 1145–1154.

(43) K. G. Lyon, G. L. Salinger, C. A. Swenson and G. K. White: *Jour. Appl. Phys.*, **48** (1977), 865–868.

(44) A. A. Khan: *Acta Cryst. -A*, **24** (1968), 403.

(45) V. A. Savastenko and A. U. Sheleg: *Phys. Stat. Solid., -A*, **48** (1978), K135–K140.

(46) A. F. Wright: *Jour. Appl. Phys.*, **82** (1997), 2833–3312.

(47) C. Deger, E. Born, H. Angerer, O. Ambacher, M. Stutzmann, J. Hornsteiner, E. Riha and G. Fischerauer: *Appl. Phys. Lett.*, **72** (1998), 2400–2402.

(48) R. B. Schwarz, K. Khachaturyan and E. R. Weber: *Appl. Phys. Lett.*, **70** (1997), 1122–1124.

(49) A. Polan, M. Grimsditch and I. Grzegory: *Jour. Appl. Phys.*, **79** (1996), 3343–3344.

(50) N. Nakamura, H. Ogi and M. Hirao: *Jour. Appl. Phys.*, **111** (2012), 013509-1–013509-6.

(51) L. E. McNeil, M. Grimsditch and R. H. French: *J. Am. Ceram. Soc.*, **76** (1993), 1132–1136.

(52) H. J. McSkimin, W. L. Bond, E. Buhler and G. K. Teal: *Phys. Rev.*, **83** (1951), 1080.

(53) J. Hall: *Phys. Rev.*, **161** (1967), 756–761.

(54) D. B. Hovis, A. Reddy and A. H. Heuer: *Appl. Phys. Lett.*, **88** (2006), 131910-1–131910-3.

(55) J. R. Gladden, J. H. So, J. D. Maynard, P. W. Saxe and Y. L. Page: *Appl. Phys. Lett.*, **85** (2004), 392–394.

(56) S. Shang, Y. Wang and Z. K. Liu: *Appl. Phys. Lett.*, **90** (2007), 101909-1–101909-3.

(57) T. B. Bateman: *Jour. Appl. Phys.*, **33** (1962), 3309–3312.

(58) T. Azuhata, M. Takesada, T. Yagi, A. Shikanai, S. F. Chichibu, K. Torii, A. Nakamura, T. Sota, G. Cantwell, D. B. Eason and C. W. Litton: *Jour. Appl. Phys.*, **94** (2003), 968–972.

(59) G. Carlotti, D. Fioretto, G. Socino and E. Verona: *Jour. Phys.: Condens. Matter.*, **7** (1995). 9147–9153.